

# A Bacterial Isolate Capable of Quenching Both Diffusible Signal Factor- and *N*-Acylhomoserine Lactone-Family Quorum Sensing Signals Shows Much Enhanced Biocontrol Potencies

Huishan Wang,<sup>#</sup> Qiqi Lin,<sup>#</sup> Lingling Dong, Wenting Wu, Zhibing Liang, Zhangyong Dong, Huijuan Ye, Lisheng Liao,<sup>\*</sup> and Lian-Hui Zhang<sup>\*</sup>



Cite This: *J. Agric. Food Chem.* 2022, 70, 7716–7726



Read Online

ACCESS |



Metrics & More



Article Recommendations



Supporting Information

**ABSTRACT:** *N*-Acylhomoserine lactone (AHL) and diffusible signal factor (DSF) molecules are two families of widely conserved quorum sensing (QS) signals. Quorum quenching (QQ) via enzymatic inactivation of QS signals is a promising strategy of biocontrol. In the search for biocontrol agent quenching both AHL and DSF signals, it has been recently identified that DSF-quenching biocontrol agent *Pseudomonas* sp. HS-18 contains at least three genes (*aigA*, *aigB*, and *aigC*) encoding AHL-acylases displaying strong AHL-acylase activities on various AHLs. Among them, AigA and AigC presented broad-spectrum enzyme activity against AHLs, while AigB preferred longer AHLs. Interestingly, transcriptional expression of *aigC* could be significantly induced by AHL signals. Heterologous expression of *aigA*–*C* in *Burkholderia cenocepacia* and *Pseudomonas aeruginosa* resulted in drastically decreased AHL accumulation, virulence factor production, biofilm formation, motility, and virulence on plants. Significantly, the two types of QQ mechanisms in HS-18 showed a strong and much desired synergistic effect for enhanced biocontrol potency against AHL- and DSF-dependent pathogens.

**KEYWORDS:** AHL, acylase, quorum quenching, DSF, *Pseudomonas* sp. HS-18

## INTRODUCTION

Quorum sensing (QS) is a kind of cell–cell communication mechanism, in which bacteria produce, release, detect, and perceive small chemical signals to sense their population density and cooperate with each other to adapt to environmental changes or to infect host organisms.<sup>1</sup> Bacteria utilize QS mechanisms to regulate a range of important cellular processes such as antibiotic production, motility, biofilm formation, genetic exchange, antimicrobial resistance, and virulence factor production, which are essential to cope with hostile environmental conditions.<sup>2,3</sup> Typically, the key components of a QS system include a chemical signal and a cognate signal receptor or biosensor kinase with a corresponding response regulator. Since the 1980s, a range of QS signals have been identified and characterized, including AHL,<sup>4</sup> AI-2,<sup>5</sup> PQS,<sup>6</sup> 3-OH PAME,<sup>7</sup> DSF,<sup>8</sup> and IQS.<sup>9</sup> Identification of these QS signals not only aids in understanding the genetic regulatory mechanisms that govern bacterial physiology and virulence, but also presents new targets and clues for developing alternative strategies against infectious diseases.

*N*-Acylhomoserine lactone (AHL) and diffusible signal factor (DSF) represent two families of the widely conserved QS signals in Gram-negative bacteria. At least over 100 bacterial species are known to produce AHL or DSF signals, respectively, and different bacterial species commonly produce various versions of AHL or DSF signals to ensure signaling specificity. Both AHL-family signals and DSF family signals are fatty acid derivatives with AHLs containing the same homoserine lactone (HSL) ring but differ in substitution at

the C-3 position and length of the acyl side chain,<sup>10</sup> and the DSF family signals sharing a fatty acid carbon chain with variations in the chain length, double-bond configuration, and side chain.<sup>11</sup> Significantly, it has become known in recent years that bacterial pathogens may employ more than one type of QS system to regulate bacterial physiology and virulence. For example, *Pseudomonas aeruginosa*, an opportunistic pathogen capable of infecting both humans and plants, relies on AHL, PQS, IQS, and DSF QS systems in modulation of virulence factor production and biofilm dispersion.<sup>3</sup> Similarly, bacterial pathogen *Burkholderia cenocepacia* employs both AHL and DSF signals in regulation of its virulence.<sup>11</sup>

Given the critical roles of QS in regulation of bacterial pathogenicity, blocking QS, which is known as quorum quenching (QQ), is regarded as a potent disease control alternative to traditional antibiotics and pesticides for impairing bacterial infections. Previous studies on QQ bacteria and QQ enzymes have showed promising potential in agricultural disease control<sup>12–14</sup> and antibiofouling applications.<sup>15</sup> The most widely studied QQ enzymes are the enzymes that hydrolyze AHL-family signals. These AHL QQ enzymes have been classified into three main types: AHL lactonases

**Received:** February 22, 2022

**Revised:** May 27, 2022

**Accepted:** May 27, 2022

**Published:** June 16, 2022



which hydrolyze the ester bond of the homoserine lactone ring of AHLs, AHL-acylases which hydrolyze the amide bond of AHLs, and AHL oxidoreductases that inactivate AHLs by oxidizing or reducing hydrogen atoms on their side chains.<sup>16</sup> Comparatively, DSF-QQ enzymes are much less studied as DSF is a relatively newly identified QS signal and there is a lack of reliable methods for screening of corresponding degradation enzymes. By developing a highly effective screening method, we recently identified a potent DSF degradation bacterial isolate *Pseudomonas* sp. HS-18, which contains multiple DSF degradation genes designated as *digA–D*.<sup>14</sup> In our attempt to search for bacterial isolates capable of inactivation more than one family of QS signals, we found that DSF-quenching strain HS-18 was able to degrade AHL signals as well. Subsequent genome sequencing analysis (GenBank accession No.: CP084413-CP084414) showed that strain HS-18 contains at least three genes encoding putative AHL-acylases designated as *AigA–C*. We then conducted substrate specificity analysis and expression pattern analysis. Moreover, the roles of these AHL-quenching genes, together with DSF-quenching genes, in disease control against two pathogens were evaluated by generation of multiple gene deletion mutants. These results highlight the impressive cumulative roles and great potential of AHL- and DSF-quenching enzymes in biocontrol of plant bacterial diseases.

## MATERIALS AND METHODS

**Bacterial Strains, Media, and Growth Conditions.** Bacterial strains and plasmids used in this study are listed in Supplementary Table S1. *E. coli* strains and *P. aeruginosa* PAO1 were grown at 37 °C. Luria Bertani (LB) medium (10 g of tryptone, 5 g of yeast extract, and 10 g of NaCl per liter; pH 7.0) was used for routine bacterial growth and maintenance. *Agrobacterium tumefaciens* strain NT1 (*traR*; *tra::lacZ749*) and *Chromobacterium violaceum* CV026 were grown at 28 °C. *Pseudomonas* sp. HS-18, *B. cenocepacia* H111, and their corresponding derived strains listed in Table S1 were grown at 30 °C. TY medium (5 g of Bacto-trypton, 3 g of yeast extract, and 6 mM CaCl<sub>2</sub> per liter; pH 7.2) was applied for bioassay using strain NT1. Where required, antibiotics were used at the following concentrations: 50 µg/mL for gentamicin and kanamycin and 100 µg/mL for ampicillin. Bacterial growth was determined by measuring optical density at a wavelength of 600 nm. Commercial AHLs were dissolved in methanol to prepare stock solutions (100 mM), respectively, including *N*-butanoyl-L-homoserine lactone (C4-HSL), *N*-hexanoyl-L-homoserine lactone (C6-HSL), *N*-(3-oxohexanoyl)-L-homoserine lactone (3-O-C6-HSL), *N*-octanoyl-L-homoserine lactone (C8-HSL), *N*-(3-hydroxy octanoyl)-L-homoserine lactone (3-OH-C8-HSL), *N*-decanoyl-L-homoserine lactone (C10-HSL), *N*-(3-hydroxy decanoyl)-L-homoserine lactone (3-OH-C10-HSL), *N*-dodecanoyl-L-homoserine lactone (C12-HSL), *N*-(3-oxododecanoyl)-L-homoserine lactone (3-O-C12-HSL), *N*-(3-hydroxy-dodecanoyl)-homoserine lactone (3-OH-C12-HSL), and *N*-(3-hydroxy-tetradecanoyl)-L-homoserine lactone (3-OH-C14-HSL) (Sigma).

**AHL Detection Assay by Biosensor Strains NT1 and CV026.** The biosensor strain *Agrobacterium tumefaciens* NT1 (*traR*; *tra::lacZ749*) was used for detection of the AHLs from C8 to C14.<sup>17</sup> Briefly, MM plates containing 5-bromo-4-chloro-3-indolyl- $\beta$ -D-galactopyranoside (X-Gal) at a final concentration of 40 µg/mL were cut into separated slices (0.8 cm in width) for further use. The bacterial overnight cultures were adjusted to OD<sub>600</sub> of 0.5 and mixed with an equal volume of fresh LB broth with addition of 50 mM MOPS and AHL at a final concentration of 10–50 µM. After incubation for 36 h, an equal volume of ethyl acetate was used to extract the culture supernatants followed by spotting 10 µL of the organic solvent containing the remaining AHL onto the top of the MM agar slice. Then the overnight cultures of biosensor NT1 were spotted at progressively further distances from the loaded samples,

with incubation at 28 °C for 24 h.<sup>17</sup> The presence of AHL might induce the expression of  $\beta$ -galactosidase in biosensor strain NT1 to display blue colonies, and the distance of blue colonies produced by NT1 is correlated with the amount of AHLs added.<sup>17</sup>  $\beta$ -Galactosidase activity was also measured with 5 µL of chloroform-treated cultures using a chemiluminescent microtiter dish assay (Tropix Galacto-Light Plus; Applied Biosystems). The assay was carried out in triplicate and repeated at least three times.

For detecting the AHLs with acyl chains shorter than six carbons, CV026 was used as the biosensor strain with a similar method applied for NT1. Briefly, LB plates were cut into separated slices (0.8 cm in width), 10 µL of the organic solvent containing the remaining AHL were spotted onto the top of the LB agar slice, and the overnight culture of CV026 was spotted at progressively further distances from the loaded samples, with incubation at 28 °C for 24 h.<sup>18</sup> The distance of the violet colonies produced by CV026 is correlated with the amount of AHLs detected.

To determine the detection of AHLs in the culture supernatants, the supernatants collected by centrifugation were extracted with ethyl acetate. The organic solvents of equal volume were then spotted onto the top of the agar slice with a biosensor on it. After incubation, the remaining AHLs were detected by using biosensor NT1 or CV026, and the relative degradation rate was derived by calculating the ratio of the distance of remaining AHL and that of the corresponding untreated AHL control.

To detect the accumulation of AHLs produced by strains H111 and PAO1 and their derivatives, 30 µL of cultures with OD<sub>600</sub> at 0.5 were added to 3 mL LB broth containing 50 mM MOPS, respectively, followed by incubation at 200 rpm for 16 h. Then the culture supernatants were collected by centrifugation and extracted with an equal volume of ethyl acetate; 2 mL of organic solvent of each sample was evaporated. To quantify C4-HSL in PAO1, 1 mL LB broth with overnight biosensor CV026 culture at a ratio of 1:100 was mixed with the evaporated organic solvent followed by incubation at 28 °C with 200 rpm shaking for 18 h. Then CV026 cells were harvested and treated with 500 µL dimethyl sulfoxide (DMSO) and centrifuged to obtain the supernatant. Detection of C4-HSL was determined by measuring the absorbance of the supernatant of lytic biosensor CV026 at 585 nm.<sup>19</sup> To quantify 3-O-C12-HSL in PAO1 and C8-HSL in H111, 1 mL TY liquid medium with overnight biosensor NT1 at a ratio of 1:100 was mixed with the evaporated organic solvent followed by incubation at 30 °C with 200 rpm shaking for 12 h. Then the  $\beta$ -galactosidase activity in biosensor NT1 induced by AHL was confirmed using the chemiluminescent microtiter dish assay as mentioned above (Tropix Galacto-Light Plus; Applied Biosystems).

**Construction of In-Frame Deletion Mutants and Complementation Strains.** All in-frame deletion (markerless) mutants of the target genes were constructed using the suicide vector pK18mob*sacB* using a homologous double crossover method as previously described.<sup>14</sup> For complementation and heterologous expression, the coding region of the gene including the predicted ribosomal binding site was amplified by polymerase chain reaction (PCR) with the primers listed in Table S2 and cloned under the control of the *lac* promoter in plasmid vector pBBR1. The PCR fragments were cloned into the vector pBBR1-MCS2 to generate corresponding expression constructs, which were then transformed into corresponding deletion mutants or wild-type strain by triparental mating with pRK2013 as mobilizing plasmid. The transformants were selected on LB agar containing 50 µg/mL kanamycin or gentamycin, and the correct complementary strains were verified by PCR and DNA sequencing.

**Liquid Chromatography–Mass Spectrometry (LC–MS) Analysis of Products Degraded by AigA–C Enzymes.** To confirm the AHL-acylase characteristic of AigA–C, overnight cultures of recombinant *E. coli* BL21(DE3) expressing *aigA–C* which were respectively carried by vector pET32a were inoculated at a ratio of 1:100 into 10 mL LB medium containing 50 mg/mL ampicillin. IPTG at 0.5 mM final concentrations was added to induce protein expression when the culture reached OD<sub>600</sub> of about 0.6–0.8. Bacterial cell pellets were harvested by centrifugation at 10,000 rpm

for 10 min and then resuspended in PBS buffer after 4 h of incubation at 37 °C with 200 rpm shaking. Bacterial cells were harvested by centrifugation and resuspended in 1 mL PBS buffer, and crude enzyme solutions were obtained after sonication and centrifugation. An aliquot of 500  $\mu$ L crude enzyme solution was mixed with 3-O-C12-HSL at a final concentration of 2 mM followed by incubation at 30 °C for 3 h with gentle shaking. The mixture was extracted with ethyl acetate. After evaporation, the samples were dissolved in 200  $\mu$ L methanol and 1  $\mu$ L sample was subjected to analysis by LC–MS using an ACQUITY UPLC HSS T3 column (1.8  $\mu$ m; 2.1 by 100 mm) with a mobile phase of 50:50 methanol–water with 0.1% formic acid (v/v) at a flow rate of 0.2 mL/min.

**Transcriptional Analysis of *aigA*–C.** Wild-type strain HS-18 was grown in LB broth supplemented with 50 mM MOPS in the presence or absence of 0.1 mM AHL at 30 °C with shaking at 200 rpm. Aliquots of cell cultures were taken at 3, 6, and 9 h after inoculation, respectively, and the cell pellets collected by centrifugation were used for purification of total RNA with the Ribopure RNA extraction kit according to the manufacturer's protocol (Ambion, Life Technologies); 400 ng of total RNA samples were taken to generate the cDNA samples using the EasyScript one-step genomic DNA (gDNA) removal and cDNA synthesis SuperMix kit according to the manufacturer's protocol (TransGen, Beijing, China). Quantitative RT-PCR (RT-qPCR) analyses of the *aig* genes were performed using a QuantStudio 6 flex system with the primer pairs listed in Table S2 and the talent qPCR PreMix (SYBR green) kit following the manufacturer's protocol (Tiangen Biotech). The constitutively expressed *rpoD* gene was used as the reference to standardize all the samples. At least three biological replicates were used for each sample, and the experiments were conducted at least twice.

**Motility Assay.** Swarming motility assays of *B. cenocepacia* H111 and its derivatives were performed on semisolid agar consisting of 0.8% tryptone, 0.5% glucose, and 0.3% agarose.<sup>20</sup> Swarming assays of *P. aeruginosa* PAO1 and its derivatives were performed on semisolid agar (1% tryptone, 0.5% NaCl, 0.35% agarose). Strains H111 and PAO1 and their derivatives at a volume of 1  $\mu$ L were respectively spotted onto the center of the agar on the plates followed by incubation for 18 h until the diameter of motility zones was measured.<sup>21</sup>

**Assay of Bacterial Biofilm Formation.** For strain H111 and its derivatives, analysis of biofilms was performed in LB broth using 96-well polypropylene microtiter dishes as mentioned above. An aliquot of 1  $\mu$ L overnight bacterial cultures with OD<sub>600</sub> at 0.5 was inoculated in 100  $\mu$ L LB broth in each well followed by incubation for 9 h at 30 °C. Then the unattached bacterial solutions were removed, and 1% crystal violet (w/v) was added for staining in each well at room temperature for 15 min followed by rinsing three times with water as described previously.<sup>13</sup> The attached bacterial cells stained by crystal violet were decolorized with 200  $\mu$ L of 95% ethanol and quantified by measuring the absorbance of the solutes at 595 nm. The assay was performed with eight individual replicates for each strain, and the experiment was repeated three times.

**Assays for Extracellular Protease Activity.** Extracellular protease activity was analyzed using the LB plate with addition of 1% skimmed milk. The diameters of clearance zones surrounding each well were measured, which were equivalent to the protease activity.<sup>22,23</sup>

**Virulence Assay.** To study the role of AHL degradation genes of HS-18 in biocontrol, virulence assay of *B. cenocepacia* H111, *P. aeruginosa* PAO1, and their derivatives was performed on onion, cabbage, and lettuce, respectively, as indicated. Onion scales were wounded on the interior surface with a sterile pipette tip; 20  $\mu$ L of bacterial culture at OD<sub>600</sub> of 1.0 were inoculated into the wound, and then onion scales were incubated at 30 °C for 3 days until the maceration zone was observed.<sup>24</sup> Twenty microliters of PAO1 culture and its derivatives at OD<sub>600</sub> of 1.0 were injected into the midribs of fresh romaine lettuce and cabbage leaves followed by incubation at 30 °C for 3 days until the soft-rot symptoms were observed.<sup>25</sup> The *aigA*–C deletion mutant 3 $\Delta$ *aig*, *digA*–D deletion mutant 4 $\Delta$ , and 4 $\Delta$ 3 $\Delta$ *aig* lacking *aigA*–C and *digA*–D genes were generated using HS-18 as the

parental strain. These mutants together with their parental strain were assayed for biocontrol patency against the AHL- and DSF-dependent pathogens H111 and PAO1. An aliquot of 20  $\mu$ L of bacterial culture at OD<sub>600</sub> about 1.0 was inoculated into the wounded plant tissues 24 h in advance; then the same amount of the bacterial pathogens was inoculated into the wounded plant tissues, respectively. After incubation for 3 days, the symptom zones of plants were photographed. The areas of the appearance of maceration zones in the pictures were estimated by measuring maceration areas using ImageJ software (version 1.52a). Then relative incidence rates of samples were considered as the relative area ratio of the symptom areas on the plant infected by pathogen derivatives or coinoculation of pathogens and biocontrol agents compared to symptom areas on the plant infected by the parental pathogens, which were designated as 100% relative incidence rate.<sup>26,27</sup>

## RESULTS

**Identification of the Genes Encoding AHL QQ Enzymes in *Pseudomonas* sp. HS-18.** Our previous study showed that the biocontrol isolate *Pseudomonas* sp. HS-18 encodes multiple DSF degradation enzymes,<sup>14</sup> which explain its potent DSF-quenching activity. In our preliminary screening to search for bacterial isolates capable of quenching both DSF and AHL signals, we found that strain HS-18 could also effectively degrade AHL signals. Computational analysis of the strain HS-18 genome revealed that there are at least three genes encoding putative AHL-acylases with over 58% similarity to other known AHL-acylases. For the convenience of discussion, these genes, that is, gene HS.18\_GM001528, HS.18\_GM001894, and HS.18\_GM005656 (Table S3), were designated as *aigA*, *aigB*, and *aigC*, respectively. AHL-acylases belong to the superfamily of Ntn-hydrolases, which include the aculeacin A acylase family, penicillin G protein family, and amidase family.<sup>28–30</sup> Domain structure analysis with the SMART program (<http://smart.embl.de>) revealed that AigA–C share similar domain structural features including a signal peptide at the N-terminal and a penicillin amidase domain (Table S3). Multiple sequence alignment and phylogenetic analyses with known AHL-acylases showed that AigA (GenBank Accession No. MW619635) is highly related to QuiP (82.29%), AigB (GenBank Accession No. MW619636) is most similar to PvdQ (58.26%), and AigC (GenBank Accession No. MW619637) shared a high similarity to HacB (76.60%) from *P. aeruginosa* PAO1, respectively (Table S3). Phylogenetic analysis showed that AigB from strain HS-18 belongs to the aculeacin A acylase family (EC 3.5.1.97), similar to the AhlM enzyme from *Streptomyces* sp. M664,<sup>31</sup> SIPVA from *Streptomyces lavendulae* ATCC 13664,<sup>32</sup> QqaR from *Deinococcus radiodurans* R1,<sup>33</sup> AiiD from *Ralstonia* sp. strain XJ12B,<sup>21</sup> Aac from *Shewanella* sp. strain MIB015,<sup>34</sup> HacA from *Pseudomonas syringae* pv. *syringae* B728a,<sup>35</sup> PvdQ from *P. aeruginosa* PAO1,<sup>36</sup> and MacQ from *Acidovorax* sp. MR-S7<sup>37</sup> (Figure 1). AigA and AigC from HS-18 belong to the penicillin G acylase protein family (EC 3.5.1.11), reminiscent of QuiP from *P. aeruginosa* PAO1, PfmA from *Pseudoalteromonas flavipulchra* JG1,<sup>29</sup> AiiC from *Anabaena* sp. strain PCC 7120,<sup>38</sup> HacB from *P. syringae* pv. *syringae* B728a,<sup>35</sup> and HacB from *P. aeruginosa* PAO1,<sup>39</sup> whereas AmiE of *Acinetobacter* sp. strain Ooi24, which is located in a different branch of phylogenetic tree, belongs to the amidase family (Figure 1).<sup>28</sup>

A typical Ntn-hydrolase superfamily protein includes an  $\alpha$ -subunit, a spacer sequence, and a  $\beta$ -subunit. Signal peptide prediction using SignalP server (<http://www.cbs.dtu.dk/services/SignalP/>) suggests that AigA–C are likely secretory



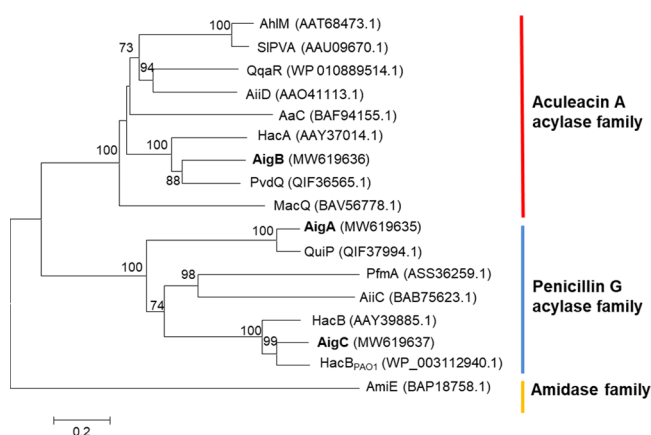


**Figure 1.** Phylogenetic analysis of AigA–C and previously characterized AHL-acylases. Phylogenetic analysis was conducted with the MEGA (version 5.05) program with neighbor-joining method (1000 bootstrap replicates) to show the phylogenetic relationship among AigA–C and the previously reported AHL-acylases (see text for references). The scale bar indicates the number of substitutions per residue. Bootstrap coefficients below 50% were not presented.

proteins with putative cleavage sites located between the amino acid positions 26 and 27, 23 and 24, and 19 and 20, respectively. Further amino acid sequence analysis of AigA–C with their characterized homologues QuiP, PvdQ, and HacB revealed that AigA–C all contain a conserved serine residue (S) (Ser-264 in AigA) as the first amino acid of the  $\beta$ -subunit which was identified as the vital catalytic site of AHL-acylases and a conserved asparagine residue (N) (Asn-265 in AigA) (Figure S1).<sup>21,37</sup> Highly variant residues isoleucine (I) (Ile-312 in AigA) and valine (V) (Val-318 in AigA) are thought to be involved in substrate specificity in various acylases, which are also conserved in AigA–C (Figure S1).<sup>21,37</sup> Taken together, the computational analysis results suggest that AigA–C enzymes are most likely functional AHL-acylases.

**Strain HS-18 Can Degrade Multiple AHLs of Different Structural Features.** Different bacterial species commonly produce AHL signals with different structural features as a way to keep signaling specificity. To determine the QQ capacity of strain HS-18 against various AHL signals, AHL signals, including C4-HSL, C6-HSL, 3-O-C6-HSL, C8-HSL, 3-OH-C8-HSL, C10-HSL, 3-OH-C10-HSL, C12-HSL, 3-O-C12-HSL, 3-OH-C12-HSL, and 3-OH-C14-HSL, were respectively evaluated using biosensors *Agrobacterium tumefaciens* NT1- (*traR*, *tra::lacZ749*) and *Chromobacterium violaceum* CV026. The biosensor *A. tumefaciens* NT1(*traR*, *tra::lacZ749*) containing *lacZ* fusion in the AHL receptor gene *tra* showed  $\beta$ -galactosidase activity induced by exogenous AHL in a concentration-dependent manner.<sup>17</sup> The biosensor *C. violaceum* CV026, a double mini-Tn5 mutant derived from ATCC 31532 (Kan<sup>R</sup>, Hg<sup>R</sup>, *cvi::Tn5xylE* and a spontaneous Str<sup>R</sup>), could produce purple violacein pigment in the presence of exogenous AHL.<sup>18</sup> The distance of the presence of blue colonies of strain NT1 or purple violacein pigment of strain CV026 is in correspondence to the amount of AHL signals which freely diffuse in the agar. The results showed that strain HS-18 displayed degradation capacity toward almost all the AHLs tested (Figure 2A). Within 12 h of reaction, C10-HSL (100%), C12-HSL (65.04%), 3-O-C12-HSL (77.6%), 3-OH-C12-HSL (100%), and 3-OH-C14-HSL (100%) were

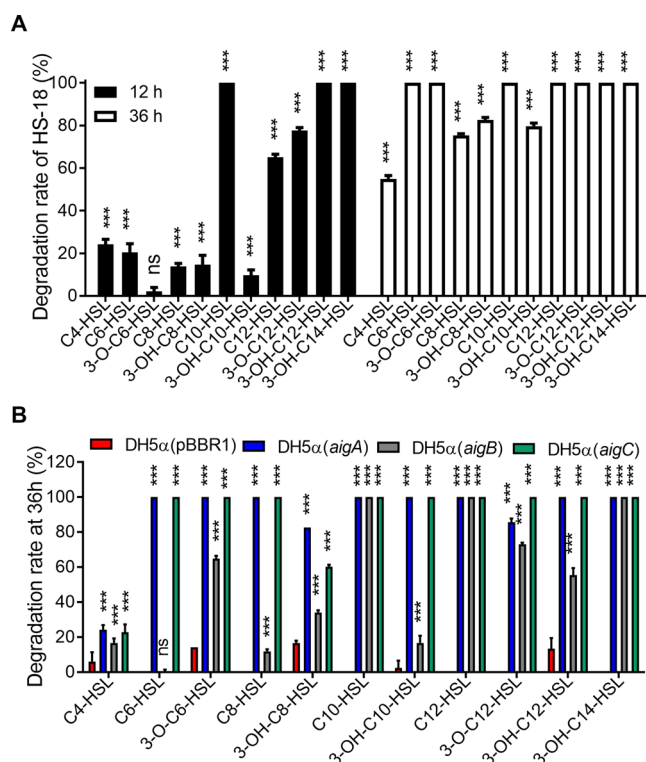


**Figure 2.** AHL QQ activity of strains HS-18, DH5 $\alpha$ (*aigA*), DH5 $\alpha$ (*aigB*), and DH5 $\alpha$ (*aigC*) on various AHLs. (A) Relative AHL degradation rates of strain HS-18 on various AHL signals at 12 h and 36 h postincubation. (B) Relative AHL degradation rates of *E. coli* strains DH5 $\alpha$ (*aigA*), DH5 $\alpha$ (*aigB*), DH5 $\alpha$ (*aigC*), and the vector control DH5 $\alpha$ (pBBR1) on various AHLs at 36 h postincubation. Bacterial strains were incubated respectively with corresponding AHL signals in LB medium containing 50 mM MOPS. The same amount of AHLs was added to the same medium as the untreated controls. After incubation, the remaining AHLs in the culture supernatants were extracted with ethyl acetate, dried, and resuspended in the same volume of methanol, respectively. The remaining AHLs were detected by using biosensor *A. tumefaciens* NT1 or *C. violaceum* CV026 as described in Methods. The relative degradation rate was derived by calculating the ratio of distance of remaining AHLs and that of the corresponding untreated AHL control. Medium- and long-chain AHLs (C8–C14) were detected by biosensor NT1(*traR*, *tra::lacZ749*) and short-chain AHLs (C4–C6) were detected by biosensor CV026. Bars indicate the mean with SD of three independent repeats. Asterisks indicate the statistical significance (\*\*\*,  $P < 0.001$ ; ns, not significant).

preferentially degraded with over 60% degradation rate, while the degradation rate of strain HS-18 toward C4-HSL (24.14%), C6-HSL (20.41%), 3-O-C6-HSL (2.13%), C8-HSL (13.90%), 3-OH-C8-HSL (14.68%), and 3-OH-C10-HSL (9.76%) is less than 30% (Figure 2A). Within 36 h of reaction, all AHLs mentioned above were degraded by strain HS-18 with over 50% degradation rate (Figure 2A). The above results indicate that strain HS-18 can degrade all AHLs but performs better with long-chain AHLs than short-chain AHLs.

**AigA–C Show Varied Substrate Preferences.** To evaluate the corresponding AHL-quenching activities of the putative AHL-acylases from strain HS-18, the *aigA–C* genes were separately cloned in the plasmid pBBR1 under the control of the *lac* promoter and expressed in *Escherichia coli* DH5 $\alpha$ , respectively. AHL degradation capacities of the three recombinant strains DH5 $\alpha$ (pBBR1-*aigA*), DH5 $\alpha$ (pBBR1-

*aigB*) and DH5 $\alpha$ (pBBR1-*aigC*) toward AHLs described above were determined using biosensors NT1(*traR*, *tra::lacZ*749) and CV026. The results showed that AigA and AigC displayed a broad-spectrum AHL degradation activity toward AHLs ranging from C4 to C14 side chains with or without 3-oxo or 3-hydroxyl substitutions (Figure 2B), whereas AigB preferred long-chain AHLs as substrates (Figure 2B).

To determine the contribution of AigA–C to the AHL degradation capacity of strain HS-18, *aigA–C* were deleted from the wild-type strain HS-18 to gain the triple-deletion mutant 3 $\Delta$ *aig*. The mutant was grown in LB medium with its parental strain HS-18 as a control, and the results showed that deletion of *aigA–C* did not affect the bacterial growth (Figure 3A). Bioassay results showed that strain HS-18 could degrade

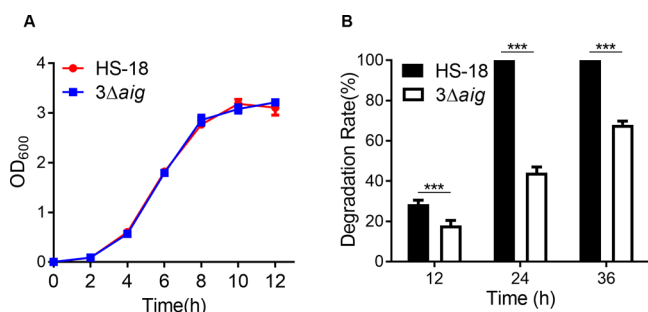


**Figure 3.** Deletion of *aigA–C* did not affect the growth of strain HS-18 but impaired its QQ activity against AHL signal. (A) Growth curve of wild-type strain HS-18 and its *aigA–C* deletion mutant 3 $\Delta$ *aig*. (B) AHL degradation assay of strain HS-18 and mutant 3 $\Delta$ *aig* in LB medium containing 25  $\mu$ M 3-O-C12-HSL. The bacterial cultures were incubated at 28  $^{\circ}$ C for 24 h prior to measurement of remaining AHL signals. LB broth containing same amount of 3-O-C12-HSL without bacterial inoculation was taken as a control. Statistical analyses were performed using the t-test and two-way analysis of variance (ANOVA). Statistics significance: \*\*\*,  $P < 0.001$ .

25  $\mu$ M 3-O-C12-HSL within 24 h, while 3 $\Delta$ *aig* showed significantly impaired AHL degradation activity (Figure 3B). Notably, deletion of *aigA–C* in strain HS-18 did not result in complete loss of AHL degradation activity compared with the blank control in which the same medium contains AHLs without bacterial inoculation (Figure 3B). It is plausible that strain HS-18 may produce other type(s) of uncharacterized AHL-quenching enzymes. Bioinformatics analysis showed that in addition to *aigA–C*, strain HS-18 genome contains nine other genes with 13–28% similarity at aa sequence level to other known AHL QQ enzymes (Table S4). Whether these are functional AHL QQ genes awaits further investigations.

**AigA–C are All AHL-Acylases.** The gene products of *aigA–C* were predicted to be AHL-acylases. To validate the enzyme property, three *aig* genes were cloned in the protein expression vector pET32a and introduced into *E. coli* strain BL21(DE3), respectively. The crude protein extracts were prepared from these recombinant strains and incubated with the QS signal 3-O-C12-HSL accordingly. MS analysis could detect the signal 3-O-C12-HSL with an M + H ion at an  $m/z$  (mass-to-charge ratio) of 298.20 (Figure 4A). The M + H ion of 3-O-C12-HSL at an  $m/z$  of 298.20 could not be detected in the reaction mixtures containing AigA–C enzymes, respectively; instead, the M + H ion at an  $m/z$  of 102.05 which corresponds to the calculated molecular ion (M + H) of homoserine lactone (HSL) (Figure 4B) was detected in all three reaction mixtures containing AigA–C enzymes (Figure

4D–F).<sup>40</sup> As a negative control, 3-O-C12-HSL was incubated with the crude protein extracts of *E. coli* BL21(DE3) containing the empty vector pET32a under the same conditions, and the MS analysis could only detect the M + H ion of 3-O-C12-HSL ( $m/z$  of 298.20) in this negative control (Figure 4C), validating that the *aigA–C* genes encode AHL-acylases, which act by hydrolyzing the amide bond of AHLs and releasing HSL and fatty acid (Figure 4G).

**Impact of Exogenous Addition of AHL on Transcriptional Expression of *aigA–C*.** To determine the effect of exogenous AHL on transcriptional expression of *aigA–C*, mRNA levels of *aigA–C* were compared in wild-type strain HS-18 grown in the presence or absence of various AHLs, that is, C6-HSL, 3-OH-C8-HSL, C10-HSL, 3-O-C12-HSL, and 3-OH-C14-HSL, at 3, 6, and 9 h after inoculation. The RT-qPCR results showed that addition of AHL did not show a significant effect on the expression of genes *aigA* and *aigB* at the three time points tested (Figure S2), which suggests that *aigA* and *aigB* are likely expressed constitutively. However, in contrast, the transcript level of *aigC* was increased significantly in response to AHL at 3 and 6 h after inoculation but dropped rapidly at 9 h postinoculation in response to long-chain AHL 3-O-C12-HSL (Figure 5A–C). The transcripts of *aigC* were about 7.6-fold, 20.9-fold, and 1.5-fold higher at 3, 6, and 9 h, respectively, in the presence of 3-O-C12-HSL postinoculation compared to the control without AHL (Figure 5A–C). These results suggest that induction of *aigC* is associated with the 3-O-C12-HSL signal.

In the QQ activity assay of AigA–C, which were expressed under the control of the *lac* promoter in *E. coli*, AigA and AigC presented stronger QQ capacity toward different AHLs than AigB (Figure 2B). We then compared the relative transcript levels of *aigA–C* in strain HS-18 using RT-qPCR analysis. The results showed that the transcript levels of *aigA* and *aigC* were significantly higher than that of *aigB* in the presence of 3-O-C12-HSL (Figure 5D). Between the constitutively expressed genes *aigA* and *aigB*, *aigA* presented higher transcript levels than *aigB*, which explains the stronger QQ capacity of AigA toward different AHLs than AigB (Figure 2B and 5D). Taken together, these findings indicate that in strain HS-18, AigA and AigC are likely the dominant QQ enzymes against AHL signals.

**Expression of *aigA–C* in *B. cenocepacia* and *P. aeruginosa* Results in Decreased Virulence Factor Production and Attenuated Bacterial Virulence.** We found that expression of *aigA–C* under the control of the *lac* promoter did not affect the growth of DSF- and AHL-dependent pathogens *B. cenocepacia* strain H111 and *P. aeruginosa* strain PAO1 (data not shown),<sup>41,42</sup> while it significantly decreased the accumulation of C8-HSL in strain H111 (Figure 6A) and reduced the levels of C4-HSL and 3-O-C12-HSL in strain PAO1 at different degrees (Figure 6B,C). The results also showed that expression of *aigA* and *aigC* in strains H111 and PAO1 presented stronger quenching activity than *aigB* on the endogenous AHL signals produced by these two bacterial pathogens (Figure 6).

The AHL-mediated virulence factor production in *B. cenocepacia* H111 and *P. aeruginosa* PAO1 was also impaired by expression of *aigA–C* (Figure 7). In *B. cenocepacia* strain H111, expression of *aigA–C* decreased the cell motility, biofilm formation, and production of extracellular protease (Figure 7A–C). Heterologous expression of *aigA–C* in *P. aeruginosa* strain PAO1 significantly reduced the bacterial cell

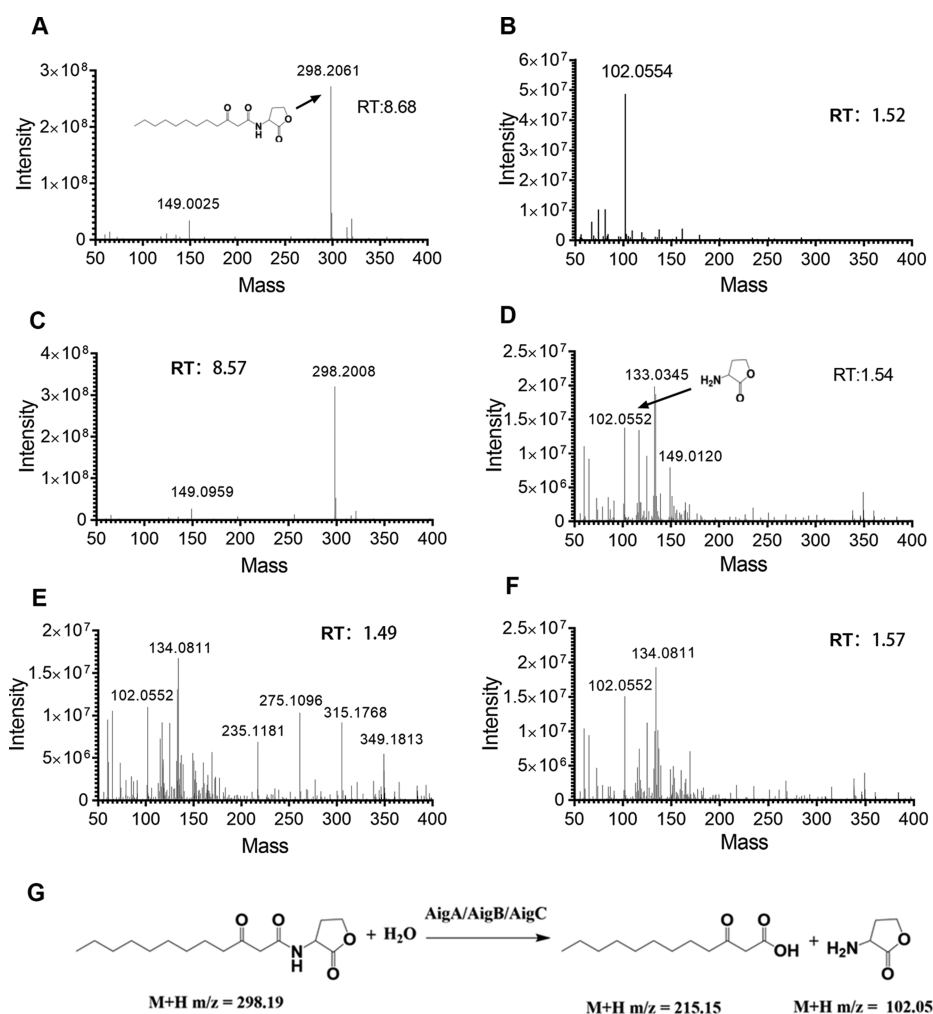


**Figure 4.** LC–MS analysis of degradation products of 3-O-C12-HSL by Aig enzymes. The MS profile of standard 3-O-C12-HSL without treatment showing the typical parental ion ( $m/z$  of  $M + H = 298.20$ ) with HPLC retention time (RT) at 8.68 min (A). The MS profile of standard HSL showing the typical parental ion ( $m/z$  of  $M + H = 102.05$ ) with HPLC RT at 1.5 min (B). The signal 3-O-C12-HSL was incubated with the protein sample from *E. coli* containing the vector as a control (C). The signal 3-O-C12-HSL was incubated with the protein samples from *E. coli* expressing *aigA* (D), *aigB* (E), and *aigC* (F), respectively. Chemical structures of 3-O-C12-HSL and its degradation products with their calculated  $M + H$   $m/z$  shown below, respectively (G). Recombinant *E. coli* BL21(DE3) expressing *aigA–C* carried by vector pET32a was induced by 0.5 mM IPTG when  $OD_{600}$  reached about 0.7, followed by incubation of 4 h at 37 °C with 200 rpm shaking. Crude enzyme solutions were obtained by sonication of the bacterial cells and 2 mM 3-O-C12-HSL was incubated with the crude enzyme solutions at 30 °C for 3 h. The mixture was then extracted with ethyl acetate, resuspended in methanol, and analyzed by LC–MS. The experiments were repeated at least twice with similar results.

motility and production of extracellular protease (Figure 7D,E). These results are consistent with the notion that decreased accumulation of endogenous AHLs caused by expression of *aigA–C* led to a reduction in virulence factor production in these AHL-dependent pathogens.

To evaluate the impact of *aigA–C* on the pathogenicity of the AHL-dependent pathogens, the three genes were introduced into *B. cenocepacia* H111 and *P. aeruginosa* PAO1, respectively, and virulence assays were then conducted using onion, lettuce, and cabbage as described previously.<sup>24,43</sup> The results revealed that strains H111(*aigA*), H111(*aigB*), and H111(*aigC*) showed a reduced maceration area on onion tissue compared to the wild-type control strain H111(pBBR1), with *aigA* presenting the most significant biocontrol effect on strain H111 (Figure 8A). Similarly, expression of *aigA–C* respectively impaired the pathogenicity of PAO1 on lettuce (Figure 8B,C) and expression of *aigA* played the most significant role in reducing the disease severity followed by *aigC* (Figure 8B,C).

### Cumulative Effect of AHL- and DSF-Quenching Enzymes on the Biocontrol Efficiency of Strain HS-18.

*Pseudomonas* sp. HS-18 was initially identified because of its remarkable DSF degradation ability.<sup>14</sup> In *B. cenocepacia* H111, DSF family signal BDSF regulates virulence factor production together with the AHL-family signal C8-HSL,<sup>42</sup> and similarly, the DSF family signal PDSF together with AHL QS signal C4-HSL and 3-O-C12-HSL coregulate the virulence traits in *P. aeruginosa* PAO1.<sup>44,45</sup> To evaluate the roles of the identified Dig and Aig QQ mechanisms in biocontrol efficiency of strain HS-18, we generated the mutant 3 $\Delta$ *aig* by deleting the AHL QQ genes *aigA–C*, the mutant 4 $\Delta$  by deleting DSF-QQ genes *digA–D*, and the mutant 4 $\Delta$ 3 $\Delta$ *aig* by deletion of *digA–D* and *aigA–C* altogether. These mutants together with its parental wild-type strain HS-18 were coinoculated with the bacterial pathogens *B. cenocepacia* H111 and *P. aeruginosa* PAO1 to determine their biocontrol efficiency on the plant models described above. The results showed that null mutation of either AHL- or DSF-QQ genes in the biocontrol strain HS-18



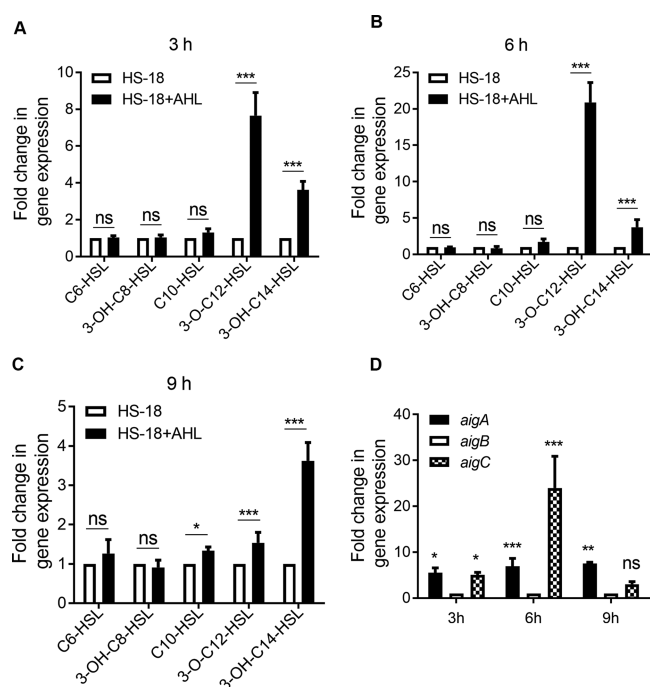


**Figure 5.** RT-qPCR analysis of *aigA*–*C* transcript levels in strain HS-18. The transcript levels of *aigC* were measured using RNA extracted from strain HS-18 grown in the presence of AHL compared to that in the absence of AHL after incubation for 3 h (A), 6 h (B), and 9 h (C). (D) Relative transcript levels of *aigA* and *aigC* were compared to that of *aigB* in the presence of AHL. The final concentration of AHL signal 3-O-C12-HSL used in this experiment was 0.1 mM. The transcript levels of the *aigA*–*C* were normalized to the housekeeping gene *rpoD*. Statistical analyses were performed using two-way ANOVA and a *t*-test. Bars indicate the mean with SD of three independent repeats. Asterisks indicate the statistical difference (\*,  $P < 0.05$ ; \*\*,  $P < 0.01$ ; \*\*\*,  $P < 0.001$ ; ns, not significant).

resulted in significantly impaired biocontrol capacities against the bacterial pathogenic strains H111 and PAO1 on onion and lettuce, respectively, compared to the wild-type strain HS-18 (Figure 8D,E). In particular, the mutant 4Δ3Δ*aig* which lacks both the *aigA*–*C* genes and the *digA*–*D* genes in strain HS-18 was least effective in suppression of disease infections caused by *B. cenocepacia* H111 and *P. aeruginosa* PAO1, respectively (Figure 8D,E).

## DISCUSSION

Bacterial pathogens commonly evolved more than one set of QS systems to regulate the expression of virulence genes. For example, the genes encoding the widely conserved AHL and DSF QS systems have been unveiled in the same genomes of quite a few bacterial pathogens, including *B. cenocepacia* and *P. aeruginosa*. In search for the QQ biocontrol agents capable of degrading both AHL and DSF signals, we found that *Pseudomonas* sp. strain HS-18, which was initially identified because of its excellent DSF-inactivation activity,<sup>14</sup> contains at least three genes designated as *aigA*, *aigB*, and *aigC* encoding putative AHL-acylases by computational analysis of the bacterial genome. Genetic and biochemical analyses validated that strain HS-18 is capable of inactivating AHL signals and that all three genes encode AHL-acylases. Among the three AHL-acylases, AigA and AigC displayed a much desired broad substrate spectrum and interestingly, transcriptional expression of *aigC* could be significantly induced by certain AHL signals. Deletion analysis showed that *aigA*–*C* contributes significantly to the AHL degradation activity of strain HS-18, but the data also suggest the presence of other uncharacterized QQ enzymes. Importantly, the findings from this study demonstrated the impressive and promising potential of a biocontrol agent capable of quenching both AHL and DSF signals in counteracting bacterial infections.

More than a dozen AHL signaling molecules have been identified in the last few decades, which vary in chain length and substitutions.<sup>4,10</sup> To date, most of the reported AHL-acylases showed a narrow substrate spectrum with a preference for long-chain AHL signals with or without substitutions at the C3 position.<sup>29,37</sup> For example, AhlM,<sup>31</sup> Aac,<sup>34</sup> PvdQ,<sup>36</sup> and QuiP<sup>46</sup> were shown to be capable of degrading AHLs with acyl chains longer than eight carbons. In our study, heterologous expression of *aigB* in *E. coli* DH5α degraded AHLs with acyl chains longer than 10 carbons more efficiently, and the substrate specificity of AigB is consistent with that of PvdQ (Table S3). It is of great interest to note that AigA and AigC possessed excellent AHL degradation capacity toward both short- and long-chain AHLs. Heterologous expression of *aigA* and *aigC* was able to inactivate all tested AHLs ranging from C4 to C14 chains with or without 3-oxo substitutions, whereas their corresponding homologues QuiP and HaeB<sub>PAO1</sub> were more selective on substrates (Table S3). Interestingly, although the substrate spectra of AigA and AigC are broader

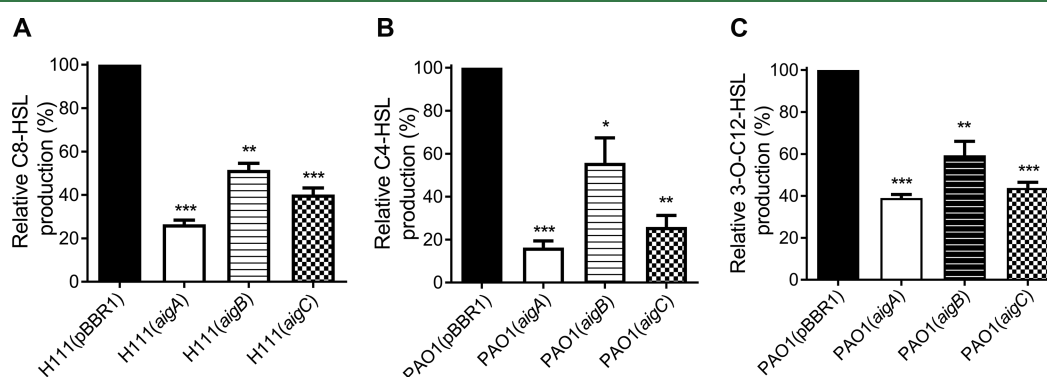


**Figure 6.** Expression of *aigA*–*C* in *B. cenocepacia* and *P. aeruginosa* reduced AHL accumulation. The *aig* genes were cloned under the control of *lac* promoter. (A) Expression of *aigA*–*C* in *B. cenocepacia* strain H111 reduced C8-HSL accumulation in culture supernatants. (B) Expression of *aigA*–*C* in *P. aeruginosa* strain PAO1 reduced accumulation of C4-HSL, and (C) 3-O-C12-HSL. Data are expressed as the mean with SD of three independent assays. Statistics significance: \*,  $P < 0.05$ ; \*\*,  $P < 0.01$ ; \*\*\*,  $P < 0.001$ .

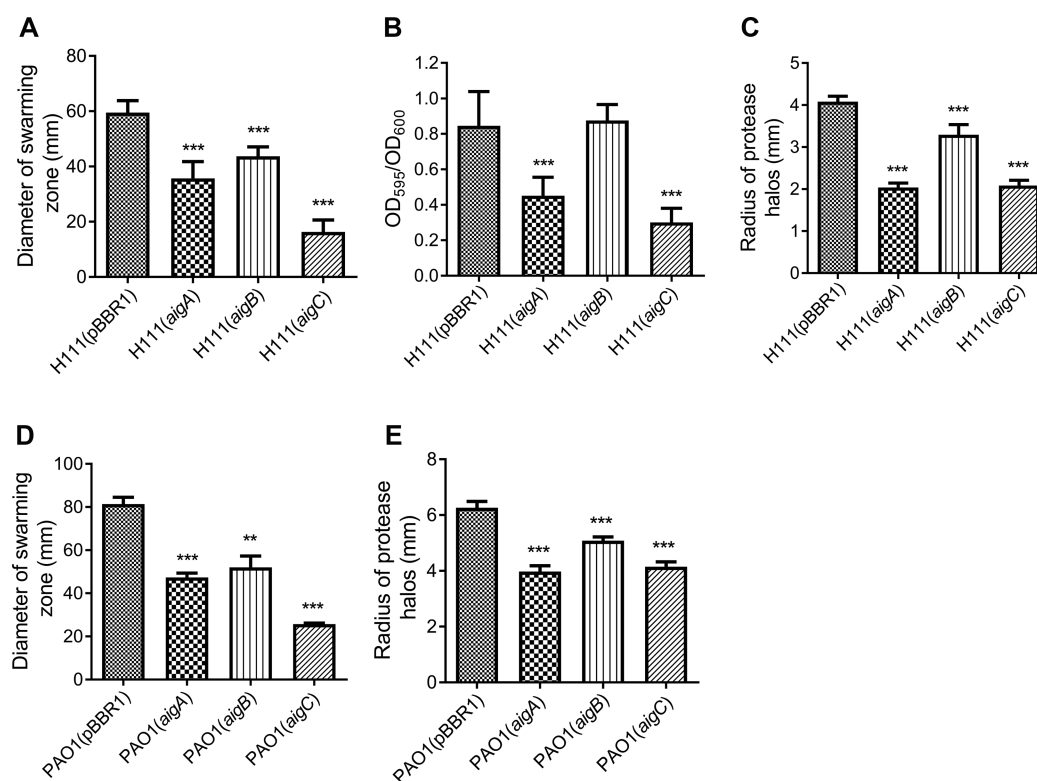


**Figure 7.** Effect of *aigA–C* on the AHL-mediated virulence traits in *B. cenocepacia* H111 and *P. aeruginosa* PAO1. Expression of *aigA–C* in strain H111 reduced its motility (A), biofilm formation (B), and extracellular protease production (C). Expression of *aigA–C* in strain PAO1 reduced swarming motility (D), and extracellular protease production (E). Statistical analyses were performed using t-test and two-way ANOVA. Data shown are the mean with SD. Statistics significance: \*,  $P < 0.05$ ; \*\*,  $P < 0.01$ ; \*\*\*,  $P < 0.001$ .

than their homologues QuiP and HacB<sub>PAO1</sub> in *P. aeruginosa* PAO1, these enzymes share the same highly variant residues Ile and Val, which are believed to be related to substrate specificity.<sup>21,37</sup> The findings seem to suggest the presence of other key variable residues in these enzymes, which might affect their substrate specificity and deserves further investigations.

An interesting feature of *Pseudomonas* sp. strain HS-18 is that its genome contains both constitutive and inducible AHL-acylase genes. Under the experimental conditions used in this study, the *aigA* and *aigB* genes were constitutively expressed, whereas the transcriptional expression of *aigC* was significantly induced by long-chain AHLs, especially 3-O-C12-HSL (Figure 5A–C). This appears reminiscent of the three genes encoding AHL-acylases in *P. aeruginosa*. A previous study showed that C10-HSL could induce the transcriptional expression of *quiP* in *P. aeruginosa* PAO1 but showed no impact or rather slight effect on the transcript levels of the genes encoding PvdQ and HacB<sub>PAO1</sub>.<sup>46</sup> While the evolutionary driving forces that coin the genes encoding constitutive and inducible AHL-acylases in these bacterial species remain unclear, it seems plausible that the presence of these enzymes of different expression patterns and substrate specificity may offer the microorganisms flexibilities in coping with various competitors in different environmental niches.

The results from this study illustrate the promising potential of exploiting a combination of different QQ mechanisms to control bacterial infections. The AHL plays a crucial role in regulating the virulence factor production in the AHL-dependent bacterial pathogens *B. cenocepacia* and *P. aeruginosa*,<sup>41,42</sup> which were selected in this study to evaluate

the potential of AigA–C against the AHL-dependent bacterial infections. *P. aeruginosa* is a notorious human pathogen,<sup>3</sup> but evidence is accumulating that it can also infect various plants, including tinda,<sup>47</sup> ginseng,<sup>48</sup> soybean,<sup>49</sup> and *Solanum lycopersicum*.<sup>50</sup> Similarly, *B. cenocepacia*, which is a member of the *Burkholderia cepacia* complex, can also infect both humans and plants.<sup>51–53</sup> These two pathogens produce and utilize AHL and DSF QS signals to regulate the production of various virulence factors during pathogen-host interaction, which are relatively well-characterized,<sup>3,41,54,55</sup> and were thus used in this study to evaluate the impact of AHL and DSF-QQ enzymes on the biocontrol potency of strain HS-18. Expression of *aigA–C* identified in this study in *P. aeruginosa* and *B. cenocepacia* significantly decreased the accumulation of endogenous AHLs, reduced the production of the AHL-dependent virulence factors, and impaired their virulence on plant models (Figures 7 and 8A–C). In particular, deletion of AHL-acylase genes *aigA–C* and DSF-inactivation genes *digA–D* together in strain HS-18 resulted in much more reduced biocontrol potency than the *aigA–C* defective mutant 3Δ*aig* and *digA–D* defective mutant 4Δ to counteract the infections by *B. cenocepacia* H111 and *P. aeruginosa* PAO1 (Figure 8D,E). These findings demonstrate the synergetic effect of the AHL- and DSF-QQ systems of strain HS-18 on the biocontrol potency against AHL- and DSF-dependent bacterial pathogens.

In summary, this study identified three AHL-acylases with differences in substrate spectrum, enzyme activity, and expression patterns. The findings not only provide useful materials for further investigation of molecular basis that govern the substrate specificity and enzyme activity of AHL-acylases, but also present intriguing clues for unveiling



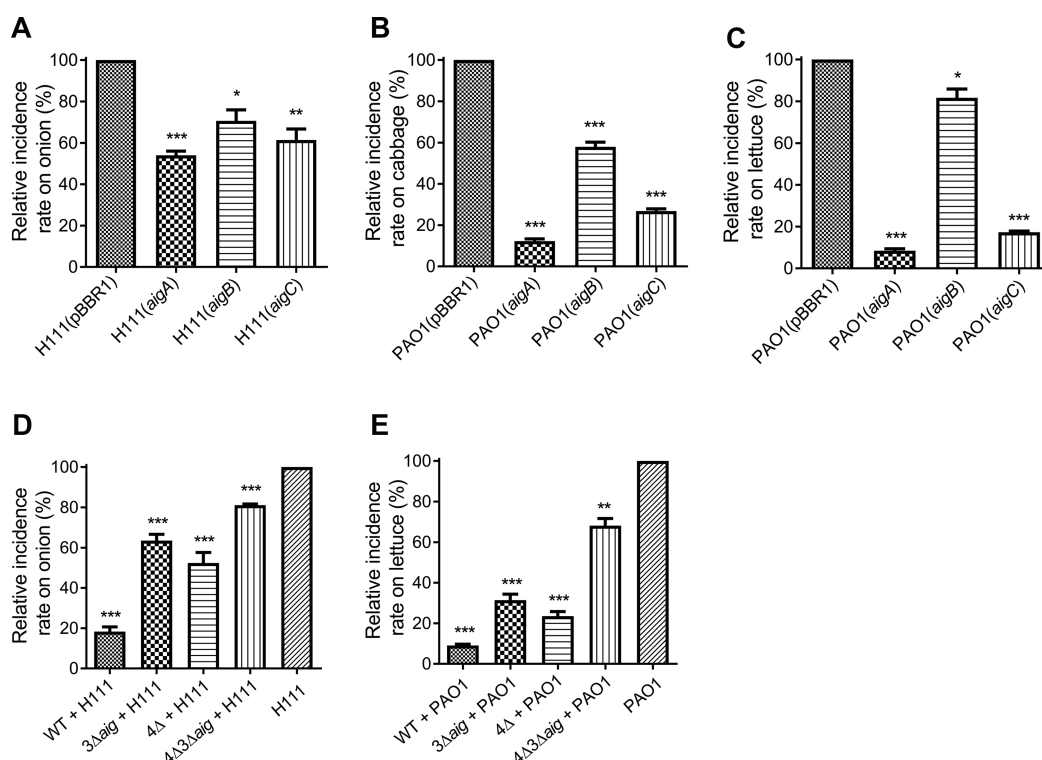


**Figure 8.** Effect of AigA–C on the pathogenicity of *B. cenocepacia* H111 and *P. aeruginosa* PAO1. Virulence of *B. cenocepacia* H111 and its derivatives on onion (A). Virulence of PAO1 and its derivatives on cabbage (B) and lettuce (C). Comparison of the biocontrol effect of *Pseudomonas* sp. strain HS-18 (WT) and its derivatives on the infections caused by *B. cenocepacia* H111 (D) and by *P. aeruginosa* PAO1 (E). The maceration area on plant tissues caused by pathogens was analyzed using ImageJ software (version 1.52a). The relative disease incidence rate was presented as the percentage of maceration area by comparison with that of corresponding wild-type pathogen. Symbol: 3Δaig, aigA–C deletion mutant in strain HS-18; 4Δ, digA–D deletion mutant in strain HS-18; 4Δ3Δaig: aigA–C and digA–D deletion mutant of strain HS-18. Statistical analyses were performed using a t-test and two-way ANOVA. Bars indicate the mean with SD. Statistical significance: \*,  $P < 0.05$ ; \*\*,  $P < 0.01$ ; \*\*\*,  $P < 0.001$ .

regulatory mechanisms and potential biological significance of AHL-inducible QQ enzymes. Most importantly, this work shows that a bacterial genome might contain various types of QQ mechanisms, which can be exploited to maximize the potency and spectrum of biocontrol agents against microbial pathogens.

## ■ ASSOCIATED CONTENT

### Supporting Information

The Supporting Information is available free of charge at <https://pubs.acs.org/doi/10.1021/acs.jafc.2c01299>.

Additional experimental details, materials, and methods, including bacteria strains, plasmids, primers, sequence alignment, substrate spectra summary, and transcriptional level analysis (PDF)

## ■ AUTHOR INFORMATION

### Corresponding Authors

**Lisheng Liao** – Guangdong Province Key Laboratory of Microbial Signals and Disease Control, Integrative Microbiology Research Centre, South China Agricultural University, Guangzhou 510642, China; Email: [lishengliao@scau.edu.cn](mailto:lishengliao@scau.edu.cn)

**Lian-Hui Zhang** – Guangdong Province Key Laboratory of Microbial Signals and Disease Control, Integrative Microbiology Research Centre, South China Agricultural University, Guangzhou 510642, China; Guangdong Laboratory for Lingnan Modern Agriculture, Guangzhou

510642, China; Institute of Plant Health, Zhongkai University of Agriculture and Engineering, Guangzhou 510225, China; Phone: +86 20 8528 8229; Email: [Lhzhang01@scau.edu.cn](mailto:Lhzhang01@scau.edu.cn)

### Authors

**Huishan Wang** – Guangdong Province Key Laboratory of Microbial Signals and Disease Control, Integrative Microbiology Research Centre, South China Agricultural University, Guangzhou 510642, China; [orcid.org/0000-0001-5378-3385](https://orcid.org/0000-0001-5378-3385)

**Qiqi Lin** – Guangdong Province Key Laboratory of Microbial Signals and Disease Control, Integrative Microbiology Research Centre, South China Agricultural University, Guangzhou 510642, China

**Lingling Dong** – Guangdong Province Key Laboratory of Microbial Signals and Disease Control, Integrative Microbiology Research Centre, South China Agricultural University, Guangzhou 510642, China

**Wenting Wu** – Guangdong Province Key Laboratory of Microbial Signals and Disease Control, Integrative Microbiology Research Centre, South China Agricultural University, Guangzhou 510642, China

**Zhibing Liang** – Guangdong Province Key Laboratory of Microbial Signals and Disease Control, Integrative Microbiology Research Centre, South China Agricultural University, Guangzhou 510642, China

Zhangyong Dong – Institute of Plant Health, Zhongkai University of Agriculture and Engineering, Guangzhou 510225, China

Huijuan Ye – Zhaoqing Food Inspection Institute, Zhaoqing, Guangdong Province 526000, China

Complete contact information is available at:

<https://pubs.acs.org/10.1021/acs.jafc.2c01299>

## Author Contributions

<sup>#</sup>H.W. and Q.L. equally contributed to this work.

## Notes

The authors declare no competing financial interest.

## ACKNOWLEDGMENTS

This work was supported by the grants from Guangdong Forestry Science and Technology Innovation Project (2018KJCX009; 2020KJCX009), the Key Realm R&D Program of Guangdong Province (2020B0202090001; 2018B020205003), Key Projects of Guangzhou Science and Technology Plan (201804020066), National Natural Science Foundation of China (31900076), and Basic Research and Applied Basic Research Program of Guangdong Province (2020A1515110111).

## REFERENCES

- (1) Mukherjee, S.; Bassler, B. L. Bacterial quorum sensing in complex and dynamically changing environments. *Nat. Rev. Microbiol.* **2019**, *17*, 371–382.
- (2) Turan, N. B.; Chormey, D. S.; Büyükpınar, Ç.; Engin, G. O.; Bakirdere, S. Quorum sensing: little talks for an effective bacterial coordination. *TrAC, Trends Anal. Chem.* **2017**, *91*, 1–11.
- (3) Ahator, S. D.; Zhang, L. Small is mighty-chemical communication systems in *Pseudomonas aeruginosa*. *Annu. Rev. Microbiol.* **2019**, *73*, 559–578.
- (4) Fuqua, C.; Parsek, M. R.; Greenberg, E. P. Regulation of gene expression by cell-to-cell communication: acyl-homoserine lactone quorum sensing. *Annu. Rev. Genet.* **2001**, *35*, 439–468.
- (5) Chen, X.; Schauder, S.; Potier, N.; Van Dorsselaer, A.; Pelczar, I.; Bassler, B. L.; Hughson, F. M. Structural identification of a bacterial quorum-sensing signal containing boron. *Nature* **2002**, *415*, 545–549.
- (6) Pesci, E. C.; Milbank, J. B.; Pearson, J. P.; McKnight, S.; Kende, A. S.; Greenberg, E. P.; Iglewski, B. H. Quinolone signaling in the cell-to-cell communication system of *Pseudomonas aeruginosa*. *Proc. Natl. Acad. Sci. U. S. A.* **1999**, *96*, 11229–11234.
- (7) Flavier, A. B.; Clough, S. J.; Schell, M. A.; Denny, T. P. Identification of 3-hydroxypalmitic acid methyl ester as a novel autoregulator controlling virulence in *Ralstonia solanacearum*. *Mol. Microbiol.* **1997**, *26*, 251–259.
- (8) Wang, L. H.; He, Y. W.; Gao, Y. F.; Wu, J. E.; Dong, Y. H.; He, C. Z.; Wang, S. X.; Weng, L. X.; Xu, J. L.; Tay, L.; Fang, R. X.; Zhang, L. H. A bacterial cell-cell communication signal with cross-kingdom structural analogues. *Mol. Microbiol.* **2004**, *51*, 903–912.
- (9) Lee, J.; Wu, J.; Deng, Y.; Wang, J.; Wang, C.; Wang, J.; Chang, C.; Dong, Y.; Williams, P.; Zhang, L. H. A cell-cell communication signal integrates quorum sensing and stress response. *Nat. Chem. Biol.* **2013**, *9*, 339–343.
- (10) Papenfort, K.; Bassler, B. L. Quorum sensing signal-response systems in gram-negative bacteria. *Nat. Rev. Microbiol.* **2016**, *14*, 576–588.
- (11) Deng, Y. Y.; Wu, J. E.; Tao, F.; Zhang, L. H. Listening to a new language: DSF-based quorum sensing in gram-negative bacteria. *Chem. Rev.* **2011**, *111*, 160–173.
- (12) Dong, Y. H.; Zhang, X. F.; Xu, J. L.; Zhang, L. H. Insecticidal *Bacillus thuringiensis* silences *Erwinia carotovora* virulence by a new form of microbial antagonism, signal interference. *Appl. Environ. Microbiol.* **2004**, *70*, 954–960.
- (13) Tettmann, B.; Niewerth, C.; Kirschhofer, F.; Neidig, A.; Dotsch, A.; Brenner-Weiss, G.; Fetzner, S.; Overhage, J. Enzyme-mediated quenching of the *Pseudomonas* quinolone signal (PQS) promotes biofilm formation of *Pseudomonas aeruginosa* by increasing iron availability. *Front. Microbiol.* **2017**, *2016*, 7.
- (14) Wang, H.; Liao, L.; Chen, S.; Zhang, L. H. A quorum quenching bacterial isolate contains multiple substrate-inducible genes conferring degradation of diffusible signal factor. *Appl. Environ. Microbiol.* **2020**, *86*, e02930–e02919.
- (15) Oh, H.; Tan, C. H.; Low, J. H.; Rzechowicz, M.; Siddiqui, M. F.; Winters, H.; Kjelleberg, S.; Fane, A. G.; Rice, S. A. Quorum quenching bacteria can be used to inhibit the biofouling of reverse osmosis membranes. *Water Res.* **2017**, *112*, 29–37.
- (16) Grandclement, C.; Tannieres, M.; Morera, S.; Dessaux, Y.; Faure, D. Quorum quenching: role in nature and applied developments. *FEMS Microbiol. Rev.* **2016**, *40*, 86–116.
- (17) Dong, Y. H.; Xu, J. L.; Li, X. Z.; Zhang, L. H. AiiA, an enzyme that inactivates the acylhomoserine lactone quorum-sensing signal and attenuates the virulence of *Erwinia carotovora*. *Proc. Natl. Acad. Sci. U. S. A.* **2000**, *97*, 3526–3531.
- (18) McClean, K. H.; Winson, M. K.; Fish, L.; Taylor, A.; Chhabra, S. R.; Camara, M.; Daykin, M.; Lamb, J. H.; Swift, S.; Bycroft, B. W.; Stewart, G.; Williams, P. Quorum sensing and *Chromobacterium violaceum*: exploitation of violacein production and inhibition for the detection of N-acylhomoserine lactones. *Microbiology* **1997**, *143*, 3703–3711.
- (19) Zhao, M.; Yu, Y.; Hua, Y.; Feng, F.; Tong, Y.; Yang, X.; Xiao, J.; Song, H. Design, synthesis and biological evaluation of N-sulfonyl homoserine lactone derivatives as inhibitors of quorum sensing in *Chromobacterium violaceum*. *Molecules* **2013**, *18*, 3266–3278.
- (20) Cui, C.; Song, S.; Yang, C.; Sun, X.; Huang, Y.; Li, K.; Zhao, S.; Zhang, Y.; Deng, Y. Disruption of quorum sensing and virulence in *Burkholderia cenocepacia* by a structural analogue of the cis-2-dodecenoic acid signal. *Appl. Environ. Microbiol.* **2019**, *85*, 8.
- (21) Lin, Y. H.; Xu, J. L.; Hu, J.; Wang, L. H.; Ong, S. L.; Leadbetter, J. R.; Zhang, L. H. Acyl-homoserine lactone acylase from *Ralstonia* strain XJ12B represents a novel and potent class of quorum-quenching enzymes. *Mol. Microbiol.* **2003**, *47*, 849–860.
- (22) Wopperer, J.; Cardona, S. T.; Huber, B.; Jacobi, C. A.; Valvano, M. A.; Eberl, L. A quorum-quenching approach to investigate the conservation of quorum-sensing-regulated functions within the *Burkholderia cepacia* complex. *Appl. Environ. Microbiol.* **2006**, *72*, 1579–1587.
- (23) Taha, M. N.; Saafan, A. E.; Ahmedy, A.; El, G. E.; Khairalla, A. S. Two novel synthetic peptides inhibit quorum sensing-dependent biofilm formation and some virulence factors in *Pseudomonas aeruginosa* PAO1. *J. Microbiol.* **2019**, *57*, 618–625.
- (24) Lee, J.; Park, J.; Kim, S.; Park, I.; Seo, Y. S. Differential regulation of toxoflavin production and its role in the enhanced virulence of *Burkholderia gladioli*. *Mol. Plant Pathol.* **2016**, *17*, 65–76.
- (25) Pustelny, C.; Albers, A.; Büldt-Karentzopoulos, K.; Parschat, K.; Chhabra, S. R.; Cámara, M.; Williams, P.; Fetzner, S. Dioxxygenase-mediated quenching of quinolone-dependent quorum sensing in *Pseudomonas aeruginosa*. *2009*, *16* (12), 1259–1267, DOI: 10.1016/j.chembiol.2009.11.013.
- (26) Schneider, C. A.; Rasband, W. S.; Eliceiri, K. W. NIH Image to ImageJ: 25 years of image analysis. *Nat. Methods* **2012**, *9*, 671–675.
- (27) Easlon, H. M.; Bloom, A. J. Easy leaf area: automated digital image analysis for rapid and accurate measurement of leaf area. *Appl. Plant Sci.* **2014**, *2*, 7.
- (28) Ochiai, S.; Yasumoto, S.; Morohoshi, T.; Ikeda, T. AmiE, a novel N-acylhomoserine lactone acylase belonging to the amidase family, from the activated-sludge isolate *Acinetobacter* sp. strain Ooi24. *Appl. Environ. Microbiol.* **2014**, *80*, 6919–6925.
- (29) Liu, N.; Yu, M.; Zhao, Y.; Cheng, J.; An, K.; Zhang, X. H. PfmA, a novel quorum-quenching N-acylhomoserine lactone acylase from *Pseudoalteromonas flavipulchra*. *Microbiology* **2017**, *163*, 1389–1398.

- (30) Zhang, J. W.; Xuan, C. G.; Lu, C. H.; Guo, S.; Yu, J. F.; Asif, M.; Jiang, W. J.; Zhou, Z. G.; Luo, Z. Q.; Zhang, L. Q. AidB, a novel thermostable N-acylhomoserine lactonase from the bacterium *Bosea* sp. *Appl. Environ. Microbiol.* **2019**, *85*, 24.
- (31) Park, S. Y.; Kang, H. O.; Jang, H. S.; Lee, J. K.; Koo, B. T.; Yum, D. Y. Identification of extracellular N-acylhomoserine lactone acylase from a *Streptomyces* sp. and its application to quorum quenching. *Appl. Environ. Microbiol.* **2005**, *71*, 2632–2641.
- (32) Torres-Bacete, J.; Hormigo, D.; Torres-Guzman, R.; Arroyo, M.; Castillon, M. P.; Garcia, L.; Acebal, C.; de la Mata, I. Overexpression of penicillin V acylase from *Streptomyces lavendulae* and elucidation of its catalytic residues. *Appl. Environ. Microbiol.* **2015**, *81*, 1225–1233.
- (33) Koch, G.; NadalJimenez, P.; Cool, R. H.; Quax, W. J. *Deinococcus radiodurans* can interfere with quorum sensing by producing an AHL-acylase and an AHL-lactonase. *FEMS Microbiol. Lett.* **2014**, *356*, 1.
- (34) Morohoshi, T.; Nakazawa, S.; Ebata, A.; Kato, N.; Ikeda, T. Identification and characterization of N-acylhomoserine lactone-acylase from the fish intestinal *Shewanella* sp. strain MIB015. *Biosci., Biotechnol., Biochem.* **2008**, *72*, 1887–1893.
- (35) Shepherd, R. W.; Lindow, S. E. Two dissimilar N-acylhomoserine lactone acylases of *Pseudomonas syringae* influence colony and biofilm morphology. *Appl. Environ. Microbiol.* **2009**, *75*, 45–53.
- (36) Huang, J. J.; Han, J. I.; Zhang, L. H.; Leadbetter, J. R. Utilization of acyl-homoserine lactone quorum signals for growth by a soil pseudomonad and *Pseudomonas aeruginosa* PAO1. *Appl. Environ. Microbiol.* **2003**, *69*, 5941–5949.
- (37) Kusada, H.; Tamaki, H.; Kamagata, Y.; Hanada, S.; Kimura, N. A novel quorum-quenching N-acylhomoserine lactone acylase from *Acidovorax* sp. strain MR-S7 mediates antibiotic resistance. *Appl. Environ. Microbiol.* **2017**, *83*, 13.
- (38) Romero, M.; Diggle, S. P.; Heeb, S.; Camara, M.; Otero, A. Quorum quenching activity in *Anabaena* sp. PCC 7120: identification of AiiC, a novel AHL-acylase. *FEMS Microbiol. Lett.* **2008**, *280*, 73–80.
- (39) Wahjudi, M.; Papaioannou, E.; Hendrawati, O.; van Assen, A. H.; van Merkerk, R.; Cool, R. H.; Poelarends, G. J.; Quax, W. J. PA0305 of *Pseudomonas aeruginosa* is a quorum quenching acylhomoserine lactone acylase belonging to the Ntn hydrolase superfamily. *Microbiology* **2011**, *157*, 2042–2055.
- (40) Chen, C. N.; Chen, C. J.; Liao, C. T.; Lee, C. Y. A probable aculeacin A acylase from the *Ralstonia solanacearum* GMI1000 is N-acyl-homoserine lactone acylase with quorum-quenching activity. *BMC Microbiol.* **2009**, *9*, 89.
- (41) Schmid, N.; Pessi, G.; Deng, Y.; Aguilar, C.; Carlier, A. L.; Grunau, A.; Omasits, U.; Zhang, L. H.; Ahrens, C. H.; Eberl, L. The AHL- and BDSF-dependent quorum sensing systems control specific and overlapping sets of genes in *Burkholderia cenocepacia* H111. *PLoS One* **2012**, *7*, No. e49966.
- (42) Kostylev, M.; Kim, D. Y.; Smalley, N. E.; Salukhe, I.; Greenberg, E. P.; Dandekar, A. A. Evolution of the *Pseudomonas aeruginosa* quorum-sensing hierarchy. *Proc. Natl. Acad. Sci. U. S. A.* **2019**, *116*, 7027–7032.
- (43) Starkey, M.; Rahme, L. G. Modeling *Pseudomonas aeruginosa* pathogenesis in plant hosts. *Nat. Protoc.* **2009**, *4*, 117–124.
- (44) Lee, J.; Zhang, L. The hierarchy quorum sensing network in *Pseudomonas aeruginosa*. *Protein Cell* **2015**, *6*, 26–41.
- (45) Liu, L.; Li, T.; Cheng, X. J.; Peng, C. T.; Li, C. C.; He, L. H.; Ju, S. M.; Wang, N. Y.; Ye, T. H.; Lian, M.; Xiao, Q. J.; Song, Y. J.; Zhu, Y. B.; Yu, L. T.; Wang, Z. L.; Bao, R. Structural and functional studies on *Pseudomonas aeruginosa* DspI: implications for its role in DSF biosynthesis. *Sci. Rep.* **2018**, *8*, 3928.
- (46) Huang, J. J.; Petersen, A.; Whiteley, M.; Leadbetter, J. R. Identification of QuiP, the product of gene PA1032, as the second acyl-homoserine lactone acylase of *Pseudomonas aeruginosa* PAO1. *Appl. Environ. Microbiol.* **2006**, *72*, 1190–1197.
- (47) Mondal, K. K.; Mani, C.; Singh, J.; Dave, S. R.; Tipre, D. R.; Kumar, A.; Trivedi, B. M. Fruit Rot of Tinda Caused by *Pseudomonas aeruginosa*-a new report from India. *Plant Dis.* **2012**, *96*, 141.
- (48) Gao, J.; Wang, Y.; Wang, C. W.; Lu, B. H. First report of bacterial root rot of ginseng caused by *Pseudomonas aeruginosa* in China. *Plant Dis.* **2014**, *98*, 1577.
- (49) Plasencia-Márquez, O.; Corzo, M.; Martínez-Zubiaur, Y.; Rivero, D.; Devescovi, G.; Venturi, V. First report of soybean (*Glycine max*) disease caused by *Pseudomonas aeruginosa* in Cuba. *Plant Dis.* **2017**, *101*, 1950–1950.
- (50) Zhang, Z.; Yao, B.; Huang, R. First report of *Pseudomonas aeruginosa* causing basal stem rot of *Solanum lycopersicum* L. in China. *Plant Dis.* **2021**, *106*, 5.
- (51) Zhang, Y.; Liu, F.; Wang, B.; Qiu, D.; Liu, J.; Wu, H.; Cheng, C.; Bei, X.; Lu, P. First report of *Burkholderia cepacia* causing fingertip rot on banana fruit in the Guangxi province of China. *Plant Dis.* **2021**, No. PDIS05211083PDN.
- (52) You, C. P.; Xiang, M. M.; Zhang, Y. X. First report of bacterial leaf streak of *Strelitzia reginae* caused by *Burkholderia cepacia*. *Plant Dis.* **2014**, *98*, 682.
- (53) Lord, R.; Jones, A. M.; Horsley, A. Antibiotic treatment for *Burkholderia cepacia* complex in people with cystic fibrosis experiencing a pulmonary exacerbation. *Cochrane Database Syst. Rev.* **2020**, *4*, No. CD009529.
- (54) Subramoni, S.; Sokol, P. A. Quorum sensing systems influence *Burkholderia cenocepacia* virulence. *Future Microbiol.* **2012**, *7*, 1373–1387.
- (55) Wang, M.; Li, X.; Song, S.; Cui, C.; Zhang, L. H.; Deng, Y. The cis-2-dodecenoic acid (BDSF) quorum sensing system in *Burkholderia cenocepacia*. *Appl. Environ. Microbiol.* **2022**, aem0234221.